J. Math. Biol. 48, 218–242 (2004)
Digital Object Identifier (DOI):
10.1007/s00285-003-0232-8

Mathematical Biology

D. Gammack · C.R. Doering · D.E. Kirschner

Macrophage response to *Mycobacterium tuberculosis* infection

Received: 10 December 2002 / Revised version: 16 April 2003 /
Published online: 20 August 2003 –

Abstract. The immune response to *Mycobacterium tuberculosis* (Mtb) infection is the formation of multicellular lesions, or granolomas, in the lung of the individual. However, the structure of the granulomas and the spatial distribution of the immune cells within is not well understood.

In this paper we develop a mathematical model investigating the early and initial immune response to Mtb. The model consists of coupled reaction-diffusion-advection partial differential equations governing the dynamics of the relevant macrophage and bacteria populations and a bacteria-produced chemokine. Our novel application of mathematical concepts of internal states and internal velocity allows us to begin to study this unique immunological structure. Volume changes resulting from proliferation and death terms generate a velocity field by which all cells are transported within the forming granuloma. We present numerical results for two distinct infection outcomes: controlled and uncontrolled granuloma growth. Using a simplified model we are able to analytically determine conditions under which the bacteria population decreases, representing early clearance of infection, or grows, representing the initial stages of granuloma formation.

1. Introduction

Tuberculosis (TB) is an aerosol-transmitted infectious disease that accounts for approximately 1.5 million deaths per year. It has been estimated that there were 8.4 million new cases of TB in 1999 [41] and that, currently, 1/3 of the world's population is infected with *Mycobacterium tuberculosis* (Mtb) [10]. However, infection rarely leads to active disease. For most people, the body's immune response is effective in either clearing or containing the pathogen, resulting in latent infection. This usually occurs anywhere from 2–5 years after initial infection [1,4]. The

D. Gammack: Department of Microbiology and Immunology, University of Michigan Medical School, Ann Arbor, MI 49109, USA.

C.R. Doering: Department of Mathematics, University of Michigan, Ann Arbor, MI 49109, USA; Michigan Center for Theoretical Physics, University of Michigan, Ann Arbor, MI 48120, USA.

D.E. Kirschner: Department of Microbiology and Immunology, University of Michigan Medical School, Ann Arbor, MI 49109, USA.

Send offprint requests to: kirschne@umich.edu

Key words or phrases: Reaction-diffusion-advection – Granuloma – Mycobacterium tuberculosis – Internal states – Internal velocity – Immune response

immune response to Mtb is the development and maintenance of unique lesions, called granulomas, in the lung of infected individuals. Granulomas are multi-cellular spheroids, consisting of bacteria, macrophages and other immune cells. It may be that how these granulomas form and how well they function could be determinant in disease progression, i.e. latency or active disease. There is evidence that smaller solid granulomas ($<$ 3mm in size) are formed in patients whose immune system is controlling the infection. Larger, caseous granulomas ($>$ 5mm in size) are less likely to effectively contain bacterial growth and spread. Thus, granuloma size and structure may contribute to the outcome of infection [5, 7]. Reactivation of latent infection can occur if the immune system is compromised in some way, e.g. through infection with human immunodeficiency virus (HIV-1), aging, drug and alcohol abuse [9].

In any infection, the first line of defense against a pathogen is the innate immune response. The initial site of Mtb infection is the alveoli of the lung, where it comes into contact with lung macrophages and dendritic cells. Macrophages respond to bacterial infections by the process of phagocytosis: the engulfment of bacteria. These macrophages are both uninfected and unactivated, meaning that they do not contain bacteria (uninfected) and are less efficient at phagocytosis than activated macrophages [6]. Activated macrophages become efficient at phagocytosis and bacterial killing due to the presence of T cells and cytokines [8, 24, 36]. Phagocytes are attracted to sites of infection via the release of chemokines by a variety of cell types. During *Mycobacterium tuberculosis* (Mtb) infection, epithelial cells, resident macrophages, T cells and bacteria each release chemokines that promote migration of immune system cells to the infection site. Similar processes also occur in tumors, wound healing and arthritis. It is speculated that if macrophages phagocytose and kill bacteria quickly, infection can conceivably be cleared [32, 38]. However, Mtb has evolved to resist killing by unactivated macrophages. In fact, it prefers to reproduce within macrophages [21]. The intracellular bacteria population of its host macrophage can become so large that the macrophage bursts and dies [38]. Therefore, a more forceful response is required and adaptive immunity develops. Infected macrophages release various chemokines (e.g. IL-8, MIP2, IP-10, MCP-1) that attract macrophages, neutrophils and T cells to sites of infection [13]. Additionally, macrophages produce cytokines (e.g. IL-12, TNF-α) that both up- and down-regulate adaptive immunity [9].

In this paper we develop a model of the innate immune response to Mtb infection. We wish to capture migration of uninfected macrophages to the site of infection and their subsequent phagocytosis of bacteria. Macrophage movement to the site of infection occurs via both random motion and directed cell movement (chemotaxis) due to chemokines released by bacteria. For example, Sannoyima *et al.* [30] discovered that fMet-Leu-Phe is one of the proteins released by bacteria that is a known chemoattractant. Once in the lung, macrophages phagocytose bacteria. Infected macrophages are able to kill their intracellular bacteria. However, their killing capacity is much lower than that for macrophages activated via T cell and cytokine signals. In fact, chronically infected macrophages are known to be less effective at a variety of immune functions. For example, infected macrophages have diminished phagocytic potential, a decreased level of MHC-II presentation (which

plays an important role in macrophage activation) [6] and produce less chemokines than activated macrophages [20,31].

Phagocytosis can be divided into two main operations: engulfment and killing. The macrophage first uses its receptors to bind to the bacteria, surrounding it by a membrane and then internalizing it into a compartment called a phagosome. Within the macrophage, lysosomes, which contain enzymes, peptides and proteins, can then fuse with the phagosome to generate a phagolysosome. The lysosomal contents are then released, killing the bacteria. Mtb, however, interferes with phagosome-lysosome fusion and thus survives in the phagosome [3] and grows in the host macrophage [21].

Previous mathematical models have been developed to consider macrophage dynamics, for example: partial differential equation (PDE) models in tumor biology [25,26]; ordinary differential equation (ODE) models in Mtb infection [42], phagocytosis [37], HIV infection [16,43] and in the immune response to an unspecified disease or infection [18,29]. The Mtb-immune system model of Wigginton and Kirschner [42] and Tran *et al.*'s [37] model of phagocytosis serve as our background models for the immune response and phagocytosis, respectively. Wigginton and Kirschner developed a model of the adaptive, cell-mediated immune response to Mtb infection. This model consisted of ODEs governing the temporal dynamics of extracellular and intracellular bacteria, relevant macrophage classes, T cells and cytokines. Simulations showed that different disease trajectories (active disease, latency and clearance) could be obtained depending on the effectiveness of macrophages and T cell killing of infected macrophages. Tran *et al.* developed a model of phagocytosis using an internal state formulation: AM_i denoted the population of alveolar macrophages (AM) containing i particles. As a macrophage engulfs more particles, the total number of internal particles increases i.e. $AM_i \rightarrow AM_{i+1} \rightarrow AM_{i+2} \ldots$ etc. That paper presented a model framework to represent various processes leading to silicosis, a disease which affects the lung and is characterized by progressive fibrosis and a chronic shortness of breath. Silicosis is caused by continued inhalation of the dust of siliceous minerals, including quartz. The model consisted of equations governing the temporal dynamics of the alveolar macrophages, neutrophils, a generic chemoattractant and fibroblasts. Using that model they were able to demonstrate quantitative agreement with experimental studies.

In addition to phagocytosis, we must capture the movement of the macrophages to the site of infection. There are many models of chemotaxis in the literature (e.g. [2,11,14,15,22,25,26,33,34]) most of which build on the original model of Keller and Segel [14]. Depending on the types of cells and biological phenomena being modeled, the chemotaxis coefficient can either be constant [25,26], dependent on the chemoattractant concentration [2,14,15,27] or dependent on cell receptors [11, 33,34]. We have not been able to find data describing how infection affects the chemotactic movement of the macrophage. We expect that they become worse at responding to chemotactic signals, as they are sick, but due to lack of data we chose the simplest option of assuming that uninfected macrophages have a constant chemotactic coefficient and that infected macrophages do not respond to chemoattractant.

Finally, the adaptive immune response to Mtb infection can lead to the formation of a granuloma [9]. Tracking the progression of the granuloma boundary will enable us to predict if infection is progressing or being contained. Mathematically, the formulation of a granuloma is similar to that of a solid tumor: both can be considered as multicellular spheroids. The models of Ward and King [39,40] use reaction-diffusion equations to study the growth of avascular tumors. They use a common internal cellular velocity, or bulk velocity, to describe the growth of the tumor radius and the movement of all cells within the tumor. It is assumed that the tumor spheroid is well packed (has no-voids) and that any cell proliferation, death or, in our case, phagocytosis contributes to a volume increase (or decrease) that causes the cells to move.

In this paper, we develop a new spatio-temporal model of the initial, innate immune response to *Mycobacterium tuberculosis* infection. Our goal is to capture either clearance by innate immunity or progression of disease via granuloma growth. In §2 we present the model and then present numerical results in §3. We find that, in agreement with experimental results, no stable latent solution is found. In §4 we present a simplified model that allows some analytical progress. Finally in §5 we discuss the model and describe additions that are required to model the complete cell-mediated immune response.

2. Mathematical model

In this section we present a mathematical model that describes the innate, initial host response to Mtb. We consider extracellular and intracellular bacteria, unactivated macrophages and a chemoattractant produced by extracellular bacteria. We use reaction-diffusion-type equations to describe how these dependent variables proliferate, die, move and interact. For simplicity, we employ a one-dimensional cartesian geometry corresponding to the growth of a slab of bacteria and immune cells rather than a spheroid. Defining $B(x,t)$ as the extracellular bacteria density, $M_w(x,t),\ w = 0,\ldots,N$ as the macrophage density (where the subscript denotes the number of intracellular bacteria within a macrophage) and the chemoattractant concentration as $C(x,t)$. Note that M_0 is the only macrophage with no internal bacteria. Below, we discuss the governing equations for each of the variables.

Extracellular bacteria dynamics

Extracellular bacteria replicate at a rate α and can be phagocytosed, at rate λ, by the first p macrophages. Essentially this means that macrophages stop eating bacteria when they become "full". Macrophages die at a rate μ at which time all intracellular bacteria are released. This is captured by the source term $\mu \sum_{w=0}^{N} w\, M_w$ in the bacteria density equation, where N is the maximal intracellular bacterial load. Intracellular bacteria replicate within their host macrophage at a rate β_w (defined below). A macrophage is able to hold up to N intracellular bacteria and if any of these N replicate, the macrophage bursts releasing bacteria extracellularly at rate $\beta_N \cdot N$. Finally, bacteria move via diffusion and a common internal velocity (for a more detailed description see Ward and King [40]). The common internal velocity

comes from models of tumor growth [40, 12] where it is assumed that a multicellular spheroid (tumor) has no voids and that processes such as cell proliferation and death generate a velocity field that moves individual cells and governs the spheroid boundary position. In our model, phagocytosis also affects the internal velocity, denoted by $v(x,t)$. Thus, the extracellular bacteria equation is:

$$\left.\begin{aligned}\frac{\partial B}{\partial t} + \overbrace{\frac{\partial (v\ B)}{\partial x}}^{\text{internal velocity}} = \overbrace{\alpha\ B}^{\text{bacterial growth}} &- \overbrace{\lambda\ B \sum_{w=0}^{p} M_w}^{\text{phagocytosis}} + \overbrace{\mu \sum_{w=0}^{N} w\ M_w}^{\text{macrophage death}} \\ &+ \underbrace{\beta_N\ N\ M_N}_{\text{macrophage bursting}} + \underbrace{D_B \frac{\partial^2 B}{\partial x^2}}_{\text{diffusion}},\end{aligned}\right\} \tag{1}$$

where D_B is the coefficient of diffusion.

Macrophage and Intracellular bacteria dynamics

As described in the introduction, macrophages have essentially three states: uninfected, infected and activated. Uninfected macrophages take up bacteria and, if not activated quickly, become infected. Infected macrophages can still phagocytose and kill, however, their ability to function properly decreases with increasing bacterial load. Activated macrophages are extremely efficient at killing their intracellular bacterial load. However, in this model of innate immunity, we do not include cytokines or T cells and therefore activated macrophages, which require T cells for activation, are not considered in the present model. The $N+1$ macrophage equations are split into two distinct types: firstly an equation for uninfected macrophages, M_0, i.e. those that have no intracellular bacteria and, secondly, a set of equations for infected macrophages, M_w, that have w intracellular bacteria. Macrophages phagocytose extracellular bacteria at a rate λ and die at a rate μ. Infected macrophages can clear their bacterial load at a rate ψ and return to the uninfected state. For simplicity, we assume that infected macrophages lose their ability to kill before they lose the ability to phagocytose. The macrophage classes included in this model are

M_0	: uninfected macrophage, can phagocytose
$M_w,\ w \in \{1, \ldots, \kappa\}$	: can phagocytose and kill
$M_w,\ w \in \{\kappa+1, \ldots, p\}$	: can phagocytose but cannot kill
$M_w,\ w \in \{p+1, \ldots, N\}$	: cannot phagocytose or kill

where $w,\ \kappa,\ p,\ N$ are positive integers and we assume that macrophages lose their ability to kill before they lose the ability to phagocytose, i.e. $\kappa < p < N$. Finally, uninfected macrophages can move via internal velocity, diffusion and by chemotaxis, i.e. up gradients of a chemokine, $C(x,t)$, produced by the extracellular

bacteria. During an actual cell-mediated immune response, macrophages themselves release chemoattractants to aid the battle against infection [9]. However, in this model we are studying solely the early response to infection, and hence we concentrate on a chemical release only by bacteria e.g. fMET-Leu-Phe [28,30]. The equation governing the dynamics of the uninfected macrophage population is given by

$$\left.\begin{aligned}\frac{\partial M_0}{\partial t} + \overbrace{\frac{\partial\,(v\;M_0)}{\partial x}}^{\text{internal velocity}} = &- \overbrace{\lambda\;B\;M_0}^{\text{phagocytosis}} - \overbrace{\mu\;M_0}^{\text{macrophage death}} + \overbrace{\psi\sum_{w=1}^{\kappa} M_w}^{\substack{\text{intracellular}\\ \text{bacterial}\\ \text{killing}}} \\ &+ \underbrace{D_M\,\frac{\partial^2 M_0}{\partial x^2}}_{\text{diffusion}} - \underbrace{\frac{\partial}{\partial x}\chi\left(M_0\,\frac{\partial C}{\partial x}\right)}_{\text{chemotaxis}}\end{aligned}\right\} \quad (2)$$

Infected macrophages, those which have internalized bacteria, are able to phagocytose extracellular bacteria while their own bacterial load $w \leq p$. They die at rate μ and can kill their intracellular bacteria if their bacterial load is $w \leq \kappa$. Intracellular bacteria can grow within their host at a rate β_w (defined below), but we assume that one bacteria divides at a time. Finally, these macrophages move via the internal velocity and diffusion only. This is probably not strictly true. We may expect that a chronically infected macrophage would have reduced speed and be less able to sense the surrounding chemical gradients, however they most likely have some potential to move chemotactically. This could be incorporated by choosing non-constant forms for D_M and χ in equations (3).

$$\left.\begin{aligned}\frac{\partial M_1}{\partial t} + \frac{\partial\,(v\;M_1)}{\partial x} = &\overbrace{-\lambda\;B\;M_1 + \lambda\;B\;M_0}^{\substack{\text{loss/gain due to}\\ \text{phagocytosis}}} - \mu\;M_1 - \psi\;M_1 \\ &- \underbrace{\beta_1\;M_1}_{\substack{\text{intracellular}\\ \text{bacteria}\\ \text{growth}}} + D_M\,\frac{\partial^2 M_1}{\partial x^2} \\ \frac{\partial M_w}{\partial t} + \frac{\partial(v\;M_w)}{\partial x} = &-\lambda_1\;B\;M_w + \lambda_2\;B\;M_{w-1} - \mu\;M_w - \psi_1 M_w \\ &\underbrace{-\beta_w\;w\;M_w + \beta_{w-1}\;(w-1)\;M_{w-1}}_{\substack{\text{loss/gain due to intracellular}\\ \text{bacteria growth}}} + D_M\,\frac{\partial\;(M_w)}{\partial x^2}\end{aligned}\right\} \quad (3)$$

Macrophages that phagocytose extracellular bacteria move "up" the infection scale i.e. $M_i \rightarrow M_{i+1}$, hence the loss and gain terms in equations (3). This process occurs

similarly with intracellular bacteria growth. Infected macrophages, with a bacterial load $w \leq \kappa$, clear this load at a rate ψ and return to the uninfected macrophage state, M_0. In the infected macrophage equation this is represented by the following form of $\psi_1(w)$

$$\psi_1(w) = \begin{cases} \psi, & w \leq \kappa \\ 0, & \text{otherwise} \end{cases}$$

Macrophages with a bacterial load $w \leq p$ can perform phagocytosis, and that rate is represented by $\lambda_1(w)$ and $\lambda_2(w)$ as follows

$$\lambda_1(w) = \begin{cases} \lambda, & w \leq p \\ 0, & \text{otherwise} \end{cases}, \qquad \lambda_2(w) = \begin{cases} \lambda, & w \leq p+1 \\ 0, & \text{otherwise.} \end{cases}$$

Finally, bacteria within macrophages grow at a rate that decreases with the number of bacteria within the host due to space and nutritional constraints. Hence, we define $\beta_w(w)$ as

$$\beta_w(w) = \frac{\beta_0}{(w_0 + w)}. \tag{4}$$

Chemoattractant dynamics

The chemoattractant $C(x,t)$ is produced by extracellular bacteria, B, at a maximal rate s_B and diffuses at a rate D_C. It has a natural decay rate, Γ_C, and is utilized by uninfected macrophages, M_0, at a rate Γ_M. The governing equation for chemoattractant, C is:

$$\frac{\partial C}{\partial t} = s_B \, \frac{B}{B + b_0} - \Gamma_C \, C - \Gamma_M \, M_0 \, C + D_C \, \frac{\partial^2 C}{\partial x^2}. \tag{5}$$

Granuloma radius

We assume that cellular velocity, $v(x,t)$ at the granuloma boundary, $x = R(t)$, describes the radial growth of the granuloma and thus the equation governing R is

$$\frac{\partial R}{\partial t} = v(R,t). \tag{6}$$

Finally, we assume that there are no voids in the granuloma, therefore, for $x \leq R(t)$

$$V_M \sum_{i=0}^{N} M_i + V_B \, B = 1, \tag{7}$$

where V_M and V_B are, respectively, the volume of a single macrophage and a single bacterium.

2.1. Non-dimensionalization

For ease of numerical analysis we non-dimensionalize equations (1)–(7). The bacteria and macrophage densities are non-dimensionalized with respect to the volume of a single bacterium (V_B) and macrophage (V_M), respectively. Time is non-dimensionalized by the bacterial growth rate (α) while the spatial coordinate, x, and the granuloma radius, $R(t)$, are non-dimensionalized with respect to the initial granuloma radius $R(t_0) = R_0$. Finally, the chemoattractant is non-dimensionalized by s_B/Γ_C. Thus, the non-dimensionalizations are written as:

$$B = \hat{B}/V_B,\ M_j = \hat{M}_j/V_M,\ t = \hat{t}/\alpha,\ x = \hat{x}\ R_0,$$

$$R = \hat{R}\ R_0,\ v = \hat{v}\ R_0\ \alpha,\ C = \hat{C}\ (s_B/\Gamma_C)$$

Now, using the non-dimensional no-voids condition (7), B is given by

$$\sum_{i=0}^{N} \hat{M}_i + \hat{B} = 1. \tag{8}$$

The non-dimensional macrophage equations are given as

$$\left.\begin{aligned}
\frac{\partial \hat{M}_0}{\partial \hat{t}} + \frac{\partial\ (\hat{v}\ \hat{M}_0)}{\partial \hat{x}} =\ & -\hat{\lambda}\ \hat{B}\ \hat{M}_0 - \hat{\mu}\ \hat{M}_0 + \hat{\psi}\ \sum_{j=1}^{\kappa} \hat{M}_j \\
& + \hat{D}_M\ \frac{\partial^2 \hat{M}_0}{\partial \hat{x}^2} - \hat{\chi}\ \frac{\partial}{\partial \hat{x}} \left(\hat{M}_0\ \frac{\partial \hat{C}}{\partial \hat{x}} \right) \\
\frac{\partial \hat{M}_1}{\partial \hat{t}} + \frac{\partial\ (\hat{v}\ \hat{M}_1)}{\partial \hat{x}} =\ & -\hat{\lambda}\ \hat{B}\ \hat{M}_1 + \hat{\lambda}\ \hat{B}\ \hat{M}_0 - \hat{\mu}\ \hat{M}_1 - \hat{\psi}\ \hat{M}_1 \\
& - \hat{\beta}_1\ \hat{M}_1 + \hat{D}_M\ \frac{\partial^2 \hat{M}_1}{\partial \hat{x}^2} \\
\frac{\partial \hat{M}_w}{\partial \hat{t}} + \frac{\partial\ (\hat{v}\ \hat{M}_w)}{\partial \hat{x}} =\ & -\hat{\lambda}_1\ \hat{B}\ \hat{M}_w + \hat{\lambda}_2\ \hat{B}\ \hat{M}_{w-1} - \hat{\mu}\ \hat{M}_w - \hat{\psi}_1 \hat{M}_w \\
& - \hat{\beta}_w\ w\ \hat{M}_w + \hat{\beta}_{w-1}\ (w-1)\ \hat{M}_{w-1} \\
& + \hat{D}_M\ \frac{\partial^2 \hat{M}_w}{\partial \hat{x}^2}
\end{aligned}\right\} \tag{9}$$

where $w = 1, \ldots, N,\ \hat{\beta}_w = \dfrac{\hat{\beta}_0}{w + w_0}$,

$$\hat{\psi}_1(w) = \begin{cases} \hat{\psi}, & w \le \kappa \\ 0, & \text{otherwise} \end{cases},$$

$$\hat{\lambda}_1(w) = \begin{cases} \hat{\lambda}, & w \le p \\ 0, & \text{otherwise} \end{cases} \quad \text{and} \quad \hat{\lambda}_2(w) = \begin{cases} \hat{\lambda}, & w \le p+1 \\ 0, & \text{otherwise.} \end{cases}$$

The non-dimensional chemoattractant equation is

$$\frac{\partial \hat{C}}{\partial \hat{t}} = \frac{\hat{B}}{\hat{B} + \hat{b_0}} - \hat{\Gamma}_C \; \hat{C} - \hat{\Gamma}_M \; \hat{M}_0 \; \hat{C} + \hat{D}_C \; \frac{\partial^2 \hat{C}}{\partial \hat{x}^2}, \tag{10}$$

and the non-dimensional granuloma radius is given by

$$\frac{\partial \hat{R}}{\partial \hat{t}} = \hat{v}(\hat{R}, \hat{t}). \tag{11}$$

Finally, using the no-voids condition, equation (8), the equation governing the internal velocity can be written as

$$\left.\begin{aligned} \hat{v}_{\hat{x}} = \hat{B} - V_r \; \hat{\lambda} \; B \; \sum_{j=0}^{N} M_j + \hat{\mu} \; \sum_{j=0}^{N} \left[\hat{M}_j \; (V_r \; j - 1)\right] \\ + \hat{\beta}_N \; N \; (V_r - 1) \; \hat{M}_N + \hat{D}_B \; \frac{\partial^2 \hat{B}}{\partial \hat{x}^2} + \hat{D}_M \; \sum_{j=0}^{N} \; \frac{\partial^2 \hat{M}_j}{\partial \hat{x}^2} \\ - \hat{\chi} \frac{\partial}{\partial \hat{x}} \left(\hat{M}_0 \; \frac{\partial \hat{C}}{\partial \hat{x}} \right) \end{aligned}\right\}, \tag{12}$$

where B is found via equation (8). The dimensionless parameters are

$$\begin{aligned} &(\hat{\lambda}, \; \hat{\lambda}_1, \; \hat{\lambda}_2) = \frac{1}{\alpha \; V_B}(\lambda, \; \lambda_1, \; \lambda_2), \; \hat{\mu} = \frac{\mu}{\alpha}, \; (\hat{\psi}, \; \hat{\psi}_1) = \frac{1}{\alpha}(\psi, \; \psi_1), \\ &\left(\hat{\beta}_w, \; \hat{\beta}_0\right) = \frac{1}{\alpha} \left(\beta_w, \; \beta_0\right), \; \hat{\Gamma}_C = \frac{\Gamma_C}{\alpha}, \; \hat{\Gamma}_M = \frac{\Gamma_M}{\alpha \; V_M}, \; \hat{b}_0 = b_0 \; V_B, \\ &\hat{V}_R = \frac{V_B}{V_M}, \; \left(\hat{D}_B, \; \hat{D}_M, \; \hat{D}_C\right) = \frac{1}{R_0^2 \; \alpha} \; (D_B, \; D_M, \; D_C), \; \hat{\chi} = \frac{\chi \; s_B}{R_0^2 \; \alpha \; \Gamma_C}. \end{aligned}$$

Boundary and Initial conditions

We impose no-flux boundary conditions at $x = 0$ for all concentration and density variables. At the granuloma boundary $x = R$, we assume that chemoattractant is released so that uninfected, M_0, macrophages are attracted into the granuloma. Therefore the boundary conditions are given as

$$\begin{aligned} \hat{D}_M \; \frac{\partial \hat{M}_w}{\partial \hat{x}} = 0, \; i = 1, \ldots, N \quad &\text{for } \hat{x} = 0, \; \hat{R} \\ \hat{D}_C \; \frac{\partial \hat{C}}{\partial \hat{x}} = 0, \; \hat{D}_M \; \frac{\partial \hat{M}_0}{\partial \hat{x}} = 0, \quad &\text{for } \hat{x} = 0 \\ \hat{D}_C \; \frac{\partial \hat{C}}{\partial \hat{x}} = -\hat{Q}_C \; \hat{C}, \quad &\text{for } \hat{x} = \hat{R} \\ \hat{D}_M \; \frac{\partial \hat{M}_0}{\partial \hat{x}} - \hat{\chi} \; \hat{M}_0 \; \frac{\partial \hat{C}}{\partial \hat{x}} = \hat{Q}_M \; \hat{C}, \; &\text{for } x = \hat{R}. \end{aligned}$$

In the above, $\hat{Q}_C = Q_C/(R_0 \; \alpha)$ and $\hat{Q}_M = Q_M \; V_M \; s_B/(\Gamma_C \; R_0 \; \alpha)$, where Q_C and Q_M are the flux rates across the granuloma boundary for the chemoattractant,

C, and the uninfected macrophages, M_0, respectively. We choose the following initial condition for the macrophages

$$\hat{M}_0(x, 0) = 0.0. \tag{13}$$

This implies that the granuloma is initially comprised of bacteria alone.

3. Numerical simulations

3.1. Numerical method

The aim of this section is to numerically approximate the solutions to the system of equations (9)–(12). We approximate the solutions in the manner described by Ward and King [40] and here we give a brief outline of this method. The moving boundary of the granuloma is mapped onto the unit interval via the following scaling of the spatial variable: $x = R(t)\ \rho$. This scaling means that the derivatives in equations (9)–(12) are also scaled:

$$\frac{\partial}{\partial t} \to \frac{\partial}{\partial t} - \frac{v(1,t)}{R(t)}\ \rho\ \frac{\partial}{\partial \rho}, \quad \frac{\partial}{\partial x} \to \frac{1}{R(t)}\frac{\partial}{\partial \rho}.$$

The equations are solved sequentially: first, $v(x, t)$ is found using the trapezium method; then $R(t)$ is updated; then equations (9)–(10) are approximated using the NAG routine D03PCF [23]. These steps are then repeated with $B(x, t)$ found at each time point by using the no-voids condition $\left(B = 1 - \sum_{i=0}^{N}\ M_i\right)$. Additionally, we need to track the total amounts of extracellular bacteria, B_T, and intracellular bacteria, I_B given by

$$\begin{aligned} B_T(t) &= \int_0^{R(t)} B(x,t)dx \\ &= R(t)\ \int_0^1 B(\rho,t)\ d\rho, \\ I_B(t) &= \int_0^{R(t)} V_R \sum_{w=0}^{N} w\ M_w(x,t)\ dx \\ &= R(t)\ \int_0^1 V_R \sum_{w=0}^{N} w\ M_w(\rho,t)\ d\rho. \end{aligned} \tag{14}$$

For simplicity, when we present levels of B_T and I_B we will use *scaled* values, namely $B_T/R(t)$ and $I_B/R(t)$ which means that the maximum values of B_T and I_B are 1 and V_R, respectively.

Parameter estimates

It is hard to determine precise values for all the parameters in this system. Hence we choose to seek order of magnitude estimates for as many parameters as possible. Such order of magnitude estimates come from both modeling and biological literature. In some cases it has not been possible to obtain more than one estimate for a

parameter, and hence we have included order of magnitude estimates for different cells so as to achieve a lower (or upper) bound. From Wigginton and Kirschner [42] (and references therein) we obtain estimates for the kinetic parameters, Owen and Sherratt [25] (and references therein) gives estimates for D_M, D_C and χ. These estimates are of similar magnitudes to the approximations used in Ward and King [39,40], Owen and Sherratt [26] and Sherratt [33]. The full list of parameter estimates is shown in Table 1. Two parameters not shown in this table are p and κ where M_p and M_κ are the last macrophages able to perform phagocytosis and kill their intracellular bacteria, respectively. It is thought that it takes between 50 and 100 intracellular bacteria to cause a macrophage to burst [42]. We do not have any data to suggest when macrophages stop ingesting bacteria or stop killing their intracellular bacteria. However, a previous study [42] has suggested that macrophages become chronically infected when they have half the number of intracellular bacteria required for bursting. It is a reasonable assumption that these macrophages have reduced phagocytic and killing ability. For simulation purposes we have chosen to take the number, N, of intracellular bacteria required to burst their host macrophage to be $N = 4$, hence we have 5 macrophage types: $M_i,\ i = 0 \ldots 4$. We choose M_2 to be the last class of phagocytic macrophage and M_1 to be the last class of macrophage able to kill its intracellular bacteria. Bacteria are, in general, much smaller than macrophages (orders of magnitude). However, due to our assumption on N, we will take (the volume of bacteria) $V_B = V_M/10$ so that a bursting number of $N_B = 4$ is reasonable. The chemoattractant decay and production terms, Γ_C, s_B, b_0, have been chosen so as to lead to reasonable results and are in line with previous authors [25,26]. The utilization of chemoattractant, Γ_M, is chosen so as to be of a reasonable size when non-dimensionalized, as there are no order of magnitude estimates available. We assume that the rate of diffusion of chemoattractant is larger than for macrophages, $D_C > D_M$, since chemoattractant is very small compared to cells in human tissue and can therefore move relatively unhindered. The assumption that the diffusion coefficient for bacteria is less than that for macrophages, $D_B < D_M$, implies that bacteria spreads out slower than macrophages. This is a reasonable assumption given that macrophages are actively patrolling the tissue looking for foreign objects. As the chemoattractant is a purely diffusive quantity, it is reasonable to assume that the flux parameter is equal to the diffusion parameter, i.e. $Q_C = D_C$. We note, however, that there is no experimental evidence to support or contradict this assumption. We have varied the resting macrophage flux parameter, Q_M, over a wide range ($10^{-16} < Q_M < 10^{-8}$). The value chosen produces both controlled and uncontrolled growth for reasonable values of ψ and β_0. Choosing Q_M much smaller requires unreasonably large values of $\psi \sim \mathcal{O}(10^3)$ to control the granuloma size.

Henceforth, for simplicity, we drop carets and assume all parameters and variables are non-dimensional, unless explicitly stated otherwise.

3.2. Numerical simulations

In this section, we first present plots showing how the granuloma radius and bacterial populations change over time for different values of ψ and β_0, the intracellular

Table 1. Dimensional Parameter values. † Values that are model specific, see description in text.

Parameter	Description	Order of Magnitude	Value used	Reference
V_M	Macrophage volume	10^{-15} m^3	10^{-15} m^3	[25,26,40]
V_B	Extracellular bacteria volume	$V_B \ll V_M$	10^{-16} m^3	Estimate
D_M	Macrophage diffusion	$10^{-9} - 10^{-15}$ m^2 s^{-1}	10^{-15} m^2 s^{-1}	[17,25,26,40]
D_B	Extracellular bacteria diffusion	$D_B < D_M$	$D_M/10$ m^2 s^{-1}	Estimate
D_C	Chemoattractant diffusion	$D_C > D_M$	$10\ D_M$	[25,26]
χ	Chemotaxis coefficient	$10^{-3} - 10^{3}$ m^2 s^{-1} M^{-1}	10^{-3} m^2 s^{-1} M^{-1}	[17,25,26,35]
Q_C	Chemoattractant flux	No data	$Q_C = D_C$	Estimate
Q_M	Uninfected macrophage flux	No data	10^{-10}	Estimate
μ	Macrophage death rate	$10^{-7} - 10^{-6}$ s^{-1}	10^{-6} s^{-1}	[25,26,42]
λ	Rate of phagocytosis	$10^{-7} - 10^{-5}$ m^{-3} s^{-1}	10^{-5} s^{-1}	[25,26,42]
ψ	Intracellular bacterial killing	10^{-14} s^{-1}	Varied	[42]
α	Extracellular bacteria growth	$0.0 - 10^{-6}$ s^{-1}	10^{-8} s^{-1}	[42]
$\beta_w = \beta_0/(w + w_0)$	Intracellular bacteria growth	$\beta_1 > \beta_2 > \ldots > \beta_N$	$w_0 = 0.01$, β_0 varied	Estimate
s_B	Source of chemoattractant	$10^{-18} - 10^{-15}$ m s^{-1}	10^{-16} m s^{-1}	Estimate
b_0	Chemoattractant half-saturation	No data	$10^{-3}\ V_B$ m^3	Estimate
Γ_C	Chemoattractant decay	No data	10^{-8} s^{-1}	Estimate
Γ_M	Chemoattractant utilization	No data	$\Gamma_C\ 10^{-14}$ m^{-3} s^{-1}	Estimate
N	Number of intracellular bacteria required to burst a host macrophage	N/A	4	Estimate†
p	last class of phagocytic macrophage	N/A	2	Estimate†
κ	last class of macrophage able to perform killing of intracellular bacteria	N/A	1	Estimate†

killing and intracellular growth parameters, respectively. Then we present graphs of the spatial distributions of the macrophage classes, velocity and chemoattractant at different time points for two specific case of: (1) controlled granuloma growth; (2) uncontrolled granuloma growth. In all the simulations that we perform, the granuloma radius either grows uncontrollably or dies out. Reasons for this are proposed in the Discussion §5. All simulations were run until the granuloma radius decreased below $R = 10^{-4}$ or increased above $R = 200$ however, for presentation purposes, we have chosen to show results up to scaled time of 6 units.

In Figure 1 we present graphs of the granuloma radius plotted against time for different values of the rate of phagocytosis, λ, the intracellular bacteria killing parameter, ψ, and the intracellular bacteria growth parameter, β_0 (Figure 1). From Figure 1(a) we see that if $\lambda = 0$ the granuloma radius grows uncontrollably, as there is no mechanism to slow the bacterial growth. However, if λ is large enough ($\lambda \sim 100$), the macrophages are able to control the extracellular bacterial population and kill the bacteria they internalize at a rate that results in clearance. It can be seen that, for $\beta_0 = 0$ and $\lambda = 100$, granuloma growth decreases as ψ increases until the value of ψ is large enough to control the granuloma, i.e. $R \to 0$ (Figure 1(b)). However, increasing β_0 from zero, and setting $\psi = 500,\ \lambda = 100$, (Figure 1(c)) increases the growth rate of the granuloma until it grows uncontrollably, which is intuitive from a biological standpoint. If ψ is large enough, less intracellular bacteria will be released than were initially taken up via phagocytosis. Therefore, there will be less extracellular bacteria, less chemokine production and a decrease in resting macrophage recruitment. However, if ψ is smaller (or β_0 large enough) there will be more extracellular bacteria and the macrophages will not be able to phagocytose and kill them rapidly enough. This will lead to the extracellular bacteria dominating the granuloma. This is shown in Figure 2 where we present graphs of the scaled bacteria populations over time for different values of ψ and β_0. We note that when the radius grows uncontrollably (for $\psi = 500,\ \beta_0 = 200$ or $\psi = 200,\ \beta_0 = 0$) the extracellular bacteria tends to one, and the intracellular bacteria dies out. This intracellular bacteria death occurs due to a lack of infected macrophages, which we discuss more fully below. When the granuloma dies out (for $\psi = 500,\ \beta_0 = 0$ or $\psi = 500,\ \beta_0 = 100$) both bacteria populations tend to zero. We have not been able to find a steady state solution for the granuloma radius, which would correspond to a state of latency. We suggest that this is probably because the steady state solution is unstable in the present model. This agrees with current biological theory, which suggests that many types of immune cells are required for successful formation of a latent granuloma.

We now discuss in more detail the cellular distributions for two cases: (1) controlled granuloma growth ($\psi = 500,\ \beta_0 = 100,\ \lambda = 100$); (2) uncontrolled granuloma growth ($\psi = 500,\ \beta_0 = 200,\ \lambda = 100$).

(1) Controlled granuloma growth: $\psi = 500,\ \beta_0 = 100,\ \lambda = 100$

Under conditions leading to the control of the granuloma, initially, the extracellular bacteria produces chemoattractant, C, recruiting uninfected macrophages, M_0, to the site of infection. By $t = 1.0$ (Figure 3(a)) the M_0 macrophages have entered the

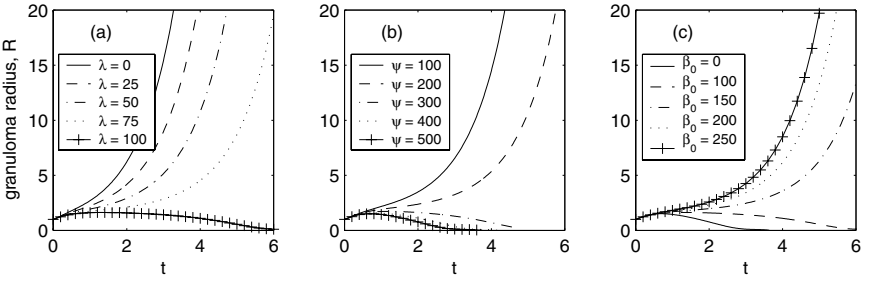

Fig. 1. Graph showing how the granuloma radius, R, varies with time, t, for: (a) $\psi = 500$, $\beta = 100$ and λ is varied; (b) $\beta_0 = 100$, $\lambda = 100$ and ψ is varied (c) $\psi = 500$, $\lambda = 100$ and β_0 is varied. Other parameters are as in Table 1.

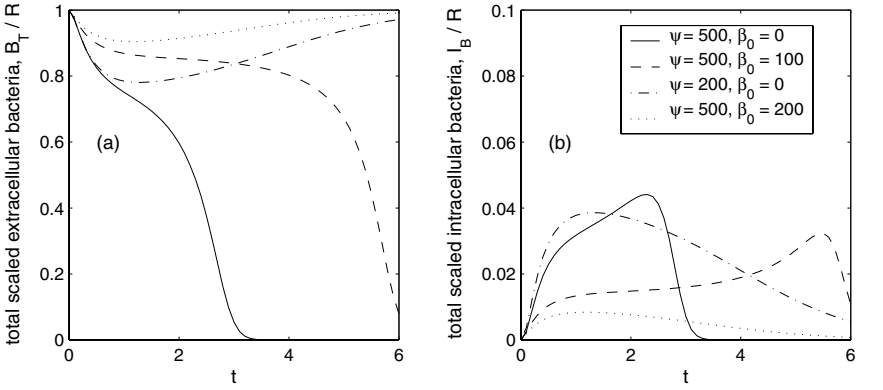

Fig. 2. Graph showing the scaled bacteria populations with respect to time for different values of ψ and β_0: (a) scaled extracellular bacterial population; (b) scaled intracellular bacterial population. Other parameters are as in Table 1.

granuloma and have a peak at the granuloma boundary, $\rho = 1$, where $\rho = x/R(t)$ is the rescaled spatial variable. The consequences of choosing $p = 2$ and $\kappa = 1$ is seen at this early time point: there are more M_3 and M_4 macrophages than M_2 and M_1 macrophages. The last class of macrophages that can perform phagocytosis are the M_2 population, whereas the last class of macrophages that can kill their intracellular bacteria are the M_1 population. This implies that the M_3 can only decrease in number via macrophage death or bacterial growth. However, M_2 macrophages can become M_3 macrophages via phagocytosis and M_1 macrophages can revert to M_0 macrophages via intracellular bacterial killing. The velocity, v, at $t = 1.0$ (Figure 4(a)) increases from $\rho = 0$, but decreases near $\rho = 1$ due to the number of macrophages. The chemoattractant, C, (Figure 4(a)) is lower at $\rho = 1$ than in the central part of the granuloma due to leakage into the surrounding tissue and being utilized by resting macrophages. The granuloma radius initially increases and does not drop in size until approximately $t = 2.0$ (Figure 1(b)) which accounts for the rise in chemoattractant between $t = 1.0$ and $t = 2.0$ (Figure 6). As the resting macrophage population rises, between $t = 2.0$ and $t = 4.0$, they become

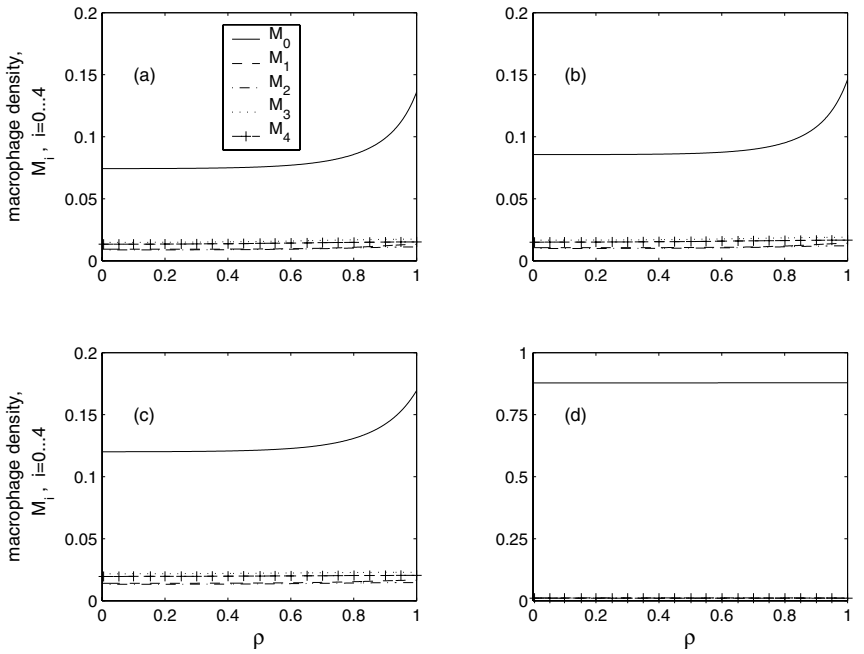

Fig. 3. Controlled granuloma growth: Graph showing the spatial distribution of the macrophage populations at different time points with $\psi = 500$, $\beta_0 = 100$ and $\lambda = 100$, other parameters are as in Table 1: (a) $t = 1.0$; (b) $t = 2.0$; (c) $t = 4.0$; (d) $t = 6.0$.

dominant throughout the granuloma. The extracellular bacteria population decreases, whereas the infected macrophage population and, hence, the intracellular bacteria populations increase due to phagocytosis. Finally, at $t = 6.0$, the infection is almost cleared: both bacterial populations and the infected macrophages are dying out; the granuloma radius, R, is decaying to zero; and the uninfected macrophages are the dominant cell type in the granuloma, $M_0(x, t) \to 1.0$.

(2) Uncontrolled granuloma growth: $\psi = 500,\ \beta_0 = 200,\ \lambda = 100$

Under conditions leading to uncontrolled granuloma growth, initially, the plots for the macrophages, velocity and chemoattractant are very similar to those for controlled growth (Figure 5(a)). However, as time progresses, the extracellular bacteria begin to dominate the granuloma due to the high intracellular growth rate inducing rapid macrophage bursting (Figures 5(b)–(d) & 2). Although more chemoattractant is released (Figure 6(b)) the macrophages do not kill their intracellular bacteria at a high enough rate to control the growth of the granuloma. Therefore, the extracellular bacteria grow uncontrollably, increasing the internal velocity of the granuloma (Figure 6(a)) and the macrophages are forced into a small layer near the granuloma boundary. As time progresses, the rate at which the granuloma grows increases ($v(R, t)$, see Figure 6(a)), the extracellular bacteria tend to one and the macrophage populations decrease.

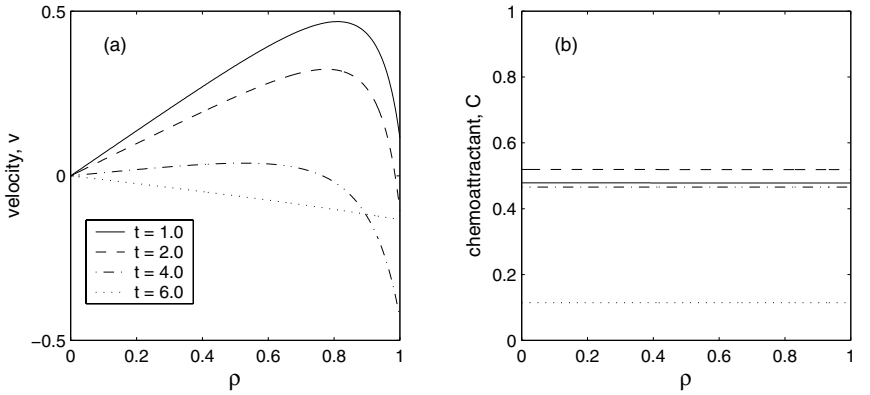

Fig. 4. Controlled granuloma growth: Graph showing the spatial distribution of (a) the internal velocity, v, and (b) the chemoattractant, C, at different time points with $\psi = 500$, $\beta_0 = 100$ and $\lambda = 100$, other parameters are as in Table 1.

Comments

The progression of Mtb infection can be split into three types of outcome: control via innate immunity (clearance); control via cell-mediated immunity (latency); uncontrolled granuloma growth with cell-mediated immunity. The model presented here is one of innate immunity as no other cell types other than resting macrophages are recruited to the site of infection. Therefore, results showing uncontrolled granuloma growth are indicators of regions in parameter space where the initial macrophage response is not sufficient to control the infection, and therefore a cell-mediated immune response is required.

4. Analysis

4.1. Spatially homogeneous model

In this section, we present a simplified version of the dimensional model presented in Section 2, equations (1),(2),(3), (5), that is spatially homogeneous. For simplicity, we assume the following: all extracellular bacteria have been phagocytosed which implies that we can neglect the equations for B and M_0, because all the bacteria is now held inside the macrophages,; macrophage natural death rate is negligible (on short time scales); and all macrophages can kill internalized bacteria ($\kappa = N$). Additionally, as all extracellular bacteria have been phagocytosed, there is no longer any production of chemokine, C. Hence, in this simplified model, the steady state value of C is $C = 0$. To asses the progression of infection over time, we track the bacterial load (i.e. the total amount of bacteria), given as

$$B_L = B_I = \sum_{1}^{N} w\ M_w(t)\ dw, \quad w = 1, \ldots, N, \tag{15}$$

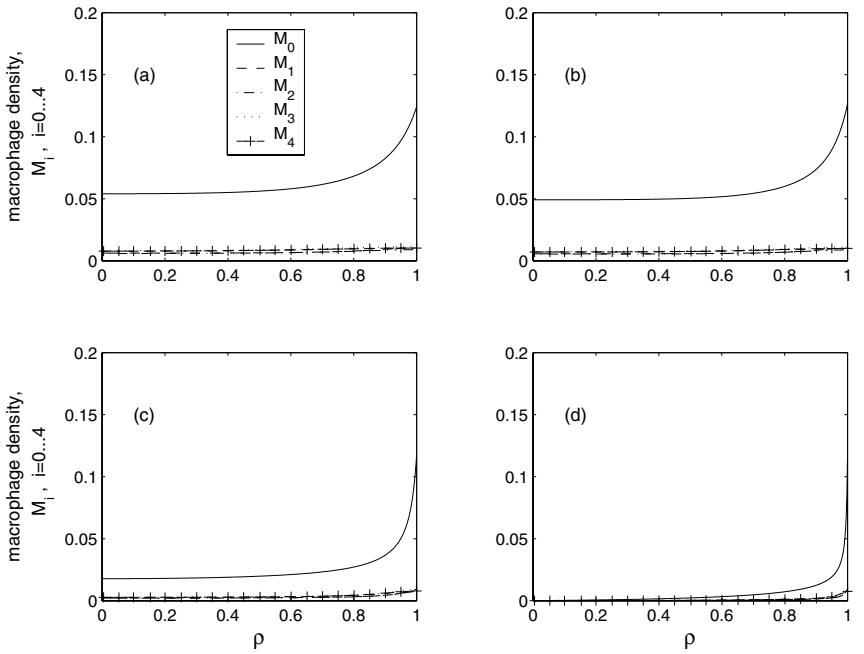

Fig. 5. Uncontrolled granuloma growth: Graph showing the spatial distribution of the macrophage populations at different time points with $\psi = 500$, $\beta_0 = 200$ and $\lambda = 100$, other parameters are as in Table 1: (a) $t = 1.0$; (b) $t = 2.0$; (c) $t = 4.0$; (d) $t = 6.0$.

and as we have assumed that there is no extracellular bacteria, $B = 0$. In equation (15), M_w represents the solution of the following dimensional equations

$$\frac{dM_w}{dt} = -\psi M_w - \beta_w\ w\ M_w + \beta_{w-1}\ (w-1)\ M_{w-1}, \quad w = 1, \ldots, N \quad (16)$$

and we have neglected all spatial effects.

Solution

We recast w, the number of intracellular bacteria in a macrophage of class M_w, as a continuous variable and solve that approximation to equation (16). Then, B_L can be written as

$$B_L = \int_1^N w\ M(w,t)\ dw \quad (17)$$

where M is the solution of the reformulated macrophage equation

$$\frac{\partial M}{\partial t}(w,t) + \frac{\partial M}{\partial w}\left(\beta_w\ w\ M(w,t)\right) = -\psi\ M(w,t) \quad (18)$$

which can be written as

$$\frac{\partial}{\partial t}M + \beta_w\ w\ \frac{\partial}{\partial w}M = -M\left(\psi + \frac{\partial}{\partial w}(\beta_w\ w)\right). \quad (19)$$

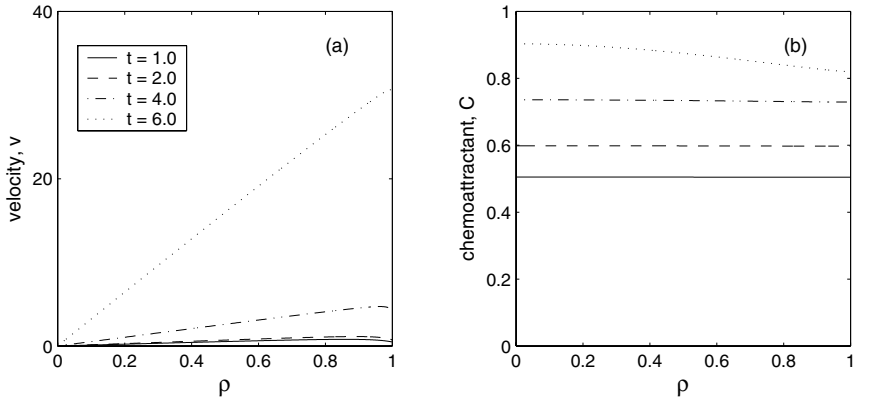

Fig. 6. Uncontrolled granuloma growth: Graph showing the spatial distribution of (a) the internal velocity, v, and (b) the chemoattractant, C, at different time points with $\psi = 500$, $\beta_0 = 200$ and $\lambda = 100$, other parameters are as in Table 1.

We take the following form of β_w, simplified from equation (4),

$$\beta_w = \beta_0 \left(1 - \frac{w}{N}\right). \tag{20}$$

Recasting this model in terms of the following non-dimensional variables and parameters

$$B = \hat{B}\ V_b^{-1},\ M = \hat{M}\ V_m^{-1},\ t = \hat{t}\ \beta_0^{-1},\ w = \hat{w}\ N,\ \psi = \hat{\psi}\ \beta_0^{-1},\ V_r = V_b/V_m,$$

leads to the following equation for M (for convenience, carets are dropped)

$$\frac{\partial M}{\partial t} + w\ (1 - w)\ \frac{\partial M}{\partial w} = -M\ (\psi + 1 - 2\ w), \tag{21}$$

where $0 \leq w \leq 1$.

Now, equation (21) can be solved using the method of characteristics. If we assume that the initial distribution of macrophages is concentrated between w_l and w_h according to

$$M(w, 0) = M_0(w) = \begin{cases} \Lambda\ (w - w_l)(w_h - w), & w_l \leq w \leq w_h \\ 0, & \text{otherwise} \end{cases} \tag{22}$$

where Λ is chosen so that $\int_{w_l}^{w_h} M(w, 0) = 1$ i.e. $\Lambda = 6/\ (w_h - w_l)^3$.
Therefore, M is given as

$$M = M_0(q)\ \left(e^{-t}\ (q - 1) - q\right)\ e^{-(\psi+1)\ t}, \tag{23}$$

where

$$q = \frac{w}{e^t - w\ (e^t - 1)}.$$

Alternatively we can write the solution for M as

$$M = \begin{cases} \Lambda\ e^{-(\psi+1)\ t} \left(w_h - \dfrac{w}{e^t - w\ a} \right) \left(\dfrac{w}{e^t - w\ a} - w_l \right) \\ \quad \times \left(1 + \dfrac{w\ a}{e^t - w\ a} \right)^2, \qquad \bar{w}_l(t) \le w \le \bar{w}_h(t) \\ \\ 0, \qquad \text{otherwise} \end{cases} \tag{24}$$

where

$$\bar{w}_h(t) = w_h\ e^t\ /(1 + a\ w_h),$$

$$\bar{w}_l(t) = w_l\ e^t\ /(1 + a\ w_l),$$

and $a = e^t - 1$.

Figure 7 shows plots of the macrophage population against intracellular bacteria for different values of t and ψ. As time progresses the bacteria divide and the macrophage population becomes "more" infected. The initial data has compact support, $M(w, 0) > 0$ only for $w \in (w_l, w_h)$, and the solution maintains compact support, $M(w, t) > 0$ only for $w \in (\bar{w}_l(t),\ \bar{w}_h(t))$. We note that $\bar{w}_h(t),\ \bar{w}_l(t) \sim 1$ as $t \to \infty$ and thus the width of the domain of compact support shrinks to zero as $t \to \infty$. Note that the unique steady state solution to equation (21) is

$$M = m_c \left(\frac{1 - w}{w} \right)^{\psi} \frac{1}{w\ (1 - w)}, \tag{25}$$

for $0 \le w \le 1$, but this is not integrable and so not an acceptable solution. Therefore, no stable steady state solution exists i.e. no stable latent state is possible. The bacterial load is found by solving equation (21), which gives the following expression for B_L

$$\left.\begin{aligned} B_L\big|_{t=0} &= V_r \frac{w_h + w_l}{2} \\ B_L\big|_{t>0} &= V_r \int_{\bar{w}_l(t)}^{\bar{w}_h(t)} w\ M\ dw \\ &= V_r\ \Lambda\ \tfrac{e^{-(\psi-1)t}}{6\ a^4} \Big\{ a\ (w_h - w_l) \Big(a^2\ (w_h - w_l)^2 \\ &\quad -3\ a\ (w_h + w_l) - 6 \Big) \\ &\quad -6 \ln \left[\tfrac{1+a\ w_l}{1+a\ w_h} \right] (1 + w_h\ a)\ (1 + w_l\ a) \Big\}. \end{aligned}\right\} \tag{26}$$

Now, we write the $B_L\big|_{t>0}$ solution as

$$B_L\big|_{t>0} = e^{-(\psi-1)\ t}\ F(t), \tag{27}$$

where,

$$F(t) = V_r \Lambda \, \frac{1}{6\,a^4} \left\{ \begin{array}{l} a\ (w_h - w_l)\Big(a^2\ (w_h - w_l)^2 \\ \quad -3\ a\ (w_h + w_l) - 6\Big) \\ -6 \ln\left[\frac{1+a\ w_l}{1+a\ w_h}\right] (1 + w_h\ a)\ (1 + w_l\ a) \end{array} \right\}. \tag{28}$$

Plots of B_L against t for various values of ψ are shown in Figure 8. It can be seen that $B_L \to 0.1 = V_r$ as $t \to \infty$ when $\psi = 0$, while for all non-zero values of ψ the bacterial load eventually decreases. Now, if $\psi = 0$, then

$$\begin{array}{rcl} \lim\limits_{a\to\infty} (1 + a)\ F(a) & = & V_r, \\ \Rightarrow \lim\limits_{t\to\infty} e^t\ F(t) & = & V_r, \end{array} \tag{29}$$

as shown in Figure 8(b). On the other hand when $\psi > 0$,

$$\lim_{t\to\infty} e^{-(\psi+t)}\ F(t) \sim \mathcal{O}\left(e^{-\psi\ t}\right). \tag{30}$$

Hence, if $\psi > 0$ then the bacterial load decreases to zero as $t \to \infty$.

From equation (21) we can obtain a lower bound on ψ such that $B_L\big|_{t=0} > B_L\big|_{t>0}$. We require

$$2\ w - 1 - \psi < 0$$

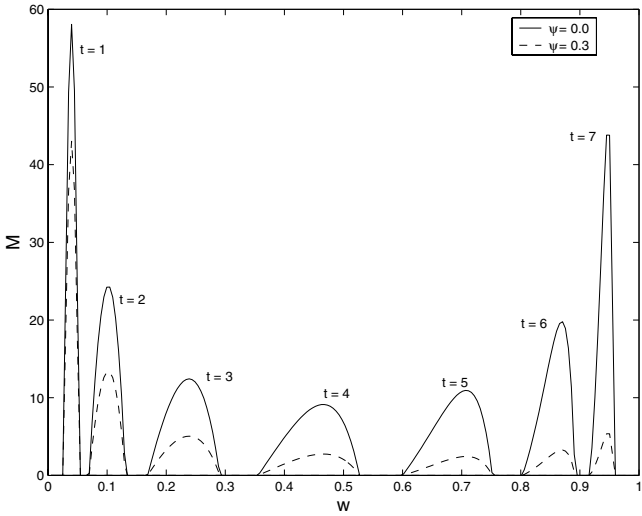

Fig. 7. Graph showing the infected macrophage population against the number of intracellular bacteria at different time points. Parameter values are $w_l = 0.01$ and $w_h = 0.02$.

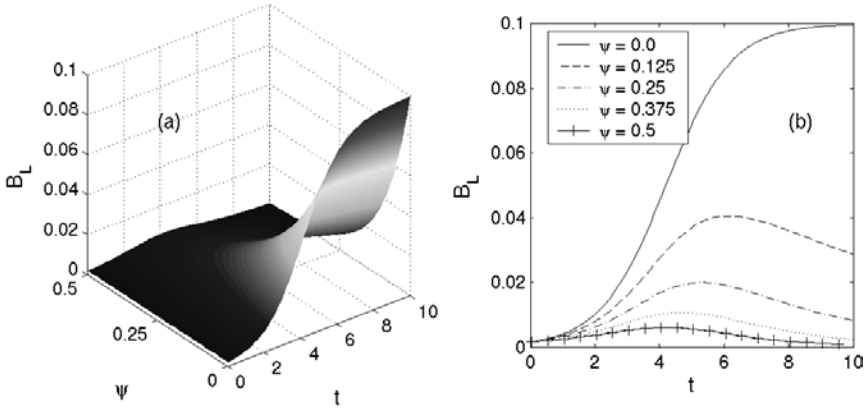

Fig. 8. Graphs showing how the bacterial load, B_L, changes with time, t, and the bacterial killing parameter, ψ: (a) three-dimensional graph; (b) two dimensional. Parameter values are $w_l = 0.01$, $w_h = 0.02$ and $V_r = 0.1$.

and as

$$\max\ w = 1,\ \forall t \geq 0 \tag{31}$$

this implies there exists a uniform (in w) lower bound on ψ such that B_L is decreasing $\forall t > 0$ and is given as $\psi = 1$.
We can obtain a more precise lower bound on ψ by analyzing the limit of $\partial B_L/\partial t$ at $t = 0.0$ and finding the value of ψ such that

$$\frac{\partial B_L}{\partial t} \leq 0.$$

For the initial data in equation (22), we find that, in order for $\partial B_L/\partial t\big|_{t=0} \leq 0$, ψ must satisfy

$$\psi \geq \frac{1}{5}\left(\frac{5\ (w_h + w_l) - 3\ \left(w_h^2 - w_l^2\right) - 4\ w_h\ w_l}{w_h + w_l}\right). \tag{32}$$

Figure 9 shows three of the curves from Figure 8 plus the curves where $\psi = 1$ and $\psi = 0.9846$ (which is the approximate value of ψ from equation (32) for the parameters given in Figure 8). In dimensional terms, ψ is the ratio of the rate of intracellular bacteria killing to the maximal rate of intracellular bacterial growth. Therefore, in dimensional terms, we find that if

$$\psi > 0.9846\ \beta_0, \tag{33}$$

the bacterial load will decrease i.e. $\psi/\beta_0 > 1$, approximately. We cannot obtain a similar inequality from the numerical results due to the effects of the other parameters in the system (e.g. the rate of phagocytosis, λ) and the fact that the full model contains intracellular and extracellular bacteria. However, from Figure 1(b,c) we find that for a fixed λ, if $\psi/\beta_0 > 3$ (approximately) the granuloma radius decreases.

Therefore, our estimates of the ratio ψ/β_0 in order to ensure infection is controlled are of the same order of magnitude for both the full and simplified models.

5. Discussion

In this paper we developed a spatio-temporal model of the initial, innate immune response to *tuberculosis*. We have extended temporal models of Wigginton and Kirschner [42] and Tran *et al.* [37] to incorporate spatial effects. Our model consists of coupled reaction-diffusion-advection equations governing dynamics of macrophages (resting and infected), bacteria (extracellular and intracellular) and a bacteria-released chemokine each of which affect the final granuloma size.

In §3 we presented graphs showing the effects of three parameters: λ, the rate of phagocytosis; ψ, the rate of intracellular bacterial killing and β_0, the intracellular bacterial growth parameter. The numerical simulations show that increasing λ and ψ decreases the rate of growth of the granuloma radius, while increasing β_0 increases granuloma growth (Figure 1). In Figures 3–6, we presented graphs showing the spatial distributions of the macrophage populations, the velocity and the chemoattractant for the two types of solution found from this model: controlled and uncontrolled bacterial growth. For the controlled case, the bacteria replicate slowly enough for the macrophages to phagocytose and kill them before they can dominate and grow exponentially. In the uncontrolled case, the intracellular growth parameter has been increased and is so large that the macrophages can no longer phagocytose and kill the bacteria quickly enough. This same result is seen if the rate of phagocytosis (or intracellular bacteria killing) is decreased below a threshold. In simulations not presented, we have also investigated the effects of varying diffusion, chemo-

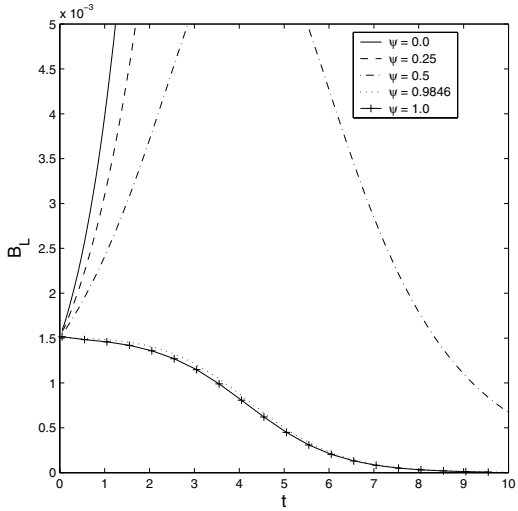

Fig. 9. Graph showing how the bacterial load, B_L, changes with time, t. The two curves that ensure that $\partial_t B_L\Big|_{t=0} \leq 0$ are also shown: $\psi = 0.9846(\cdots)$ and $\psi = 1.0(-+-)$. Parameter values are $w_l = 0.01$, $w_h = 0.02$ and $V_r = 0.1$.

taxis and flux parameters. Varying these parameters did not lead to any qualitatively different results. For example, increasing the in-flux of uninfected macrophages at the granuloma boundary (increasing Q_M) initially increased the granuloma size as more macrophages are present. Granuloma growth then slows due to more macrophages present in the granuloma that perform phagocytosis and killing.

In §4 we simplified the full model to examine the total amount of bacteria. Using this model it is possible to find a lower bound on ψ, the rate of intracellular bacteria killing, so that the total amount of bacteria decreases and therefore the infection can be controlled.

It is significant that, in the full model, we have not been able to find a stable steady state for the granuloma size. For a model that focuses solely on innate immunity this is not surprising. In fact, it is known that for a latent infection, other immune cells are required [5]. Therefore, a steady state for the granuloma radius should result from including equations for T cells and activated macrophages. Ongoing work is addressing these aspects of adaptive immunity.

In our model we assume that macrophages with less than a certain number (κ) of intracellular bacteria can phagocytose extracellular bacteria. Another approach to this would be that of Tran *et al.* [37] who developed a model such that each macrophage type, $M_i,\ i = 1 \ldots N$ (where i indicates the number of intracellular molecules), has an associated rate of phagocytosis, λ_i. They assume that the macrophage rate of phagocytosis decreases with the number of intracellular bacteria and therefore $\lambda_1 > \lambda_2 > \ldots > \lambda_N$. However, this requires estimates for the N phagocytosis parameters which, using the current literature, is not practical.

Alveolar epithelial cells produce chemokines that attract macrophages and T cells [19]. This, coupled with the fact that bacteria and macrophages also release chemokines, implies that there are more chemoattractants produced during Mtb infection that the bacteria-produced one used in the present model. It would be relatively simple to incorporate additional chemokines in the model.

In conclusion, our model provides a framework for the development of spatio-temporal models of the immune response, not just for *Mycobacterium tuberculosis*. In particular we are studying the effects of cell-mediated immunity on granuloma formation with the aim of developing a more complete description of the immune response to Mtb.

Acknowledgements. The authors thank Drs. JoAnne Flynn and John Chan for many useful discussions. DEK and DG were supported by N.I.H. grants HL6119 and HL68526. CRD was supported in part by the N.S.F. award PHY-9900635.

References

1. Bloom, B.R.: Tuberculosis: pathogenesis, protection, and control. ASM Press, Washington, DC, 1994
2. Chiu, C., Hoppensteadt, F.C.: Mathematical models and simulations of bacterial growth and chemotaxis in a diffusion gradient chamber. J. Math. Biol. **42**, 120–144 (2001)
3. Collins, H.L., Kaufmann, S.H.E.: The many faces of host responses to tuberculosis. Immunol. **103**, 1–9 (2001)
4. Comstock, G.W., Livesay, V.T., Woolpert, S.F.: The prognosis of a positive tuberculin reaction in childhood and adolescence. Am. J. Epidemiol. **99**, 131–138 (1974)

5. Dannenberg, A.M., Rook, G.S.W.: Pathogenesis of pulmonary tuberculosis: an interplay of tissue-damaging and macrophage-activating immune responses - dual mechanisms that control bacillary multiplication. In: Bloom, B.R., (ed) Tuberculosis: pathogenesis, protection, and control. ASM Press, Washington, DC, 1994
6. DesJardin, L.E., Kaufman, T.M., Potts, B., Kutzbach, B., Yi, H., Schlesinger, L.S.: Mycobacterium tuberculosis-infected human macrophages exhibit enhanced cellular adhesion with increased expression of LFA-1 and ICAM-1 and reduced expression and/or function of complement receptors, FcγRii and the mannose receptor. Microbiol. **148**, 3161–3171 (2002)
7. Emile, J.-.F, Patey, N., Altare, F., Lamhamedi, S., Jouanguy, E., Boman, F., Quillard, J., Lecomte-Houcke, M., Verola, O., Mousnier, J.-F., Dijoud, F., Blanche, S., Fischer, A., Brousse, N., Casanova, J.-L.: Correlation of granuloma structure with clinical outcome defines two types of idiopathic disseminated BCG infection. J. Pathology **181**, 25–30 (1997)
8. Flesch, I.E., Kaufmann, S.H.: Activation of tuberculostatic macrophage functions by gamma interferon, interleukin-4, and tumor necrosis factor. Infect. Immun. **58**, 2675–2677 (1990)
9. Flynn, J.L., Chan, J.: Immunology of tuberculosis. Annu. Rev. Immunol. **19**, 93–129 (2001)
10. Flynn, J.L., Chan, J.: Tuberculosis: latency and reactivation. Infect. Immun. **69**, 4195–4201 (2001)
11. Höfer, T., Sherratt, J.A., Maini, P.K.: Cellular pattern formation during Dictyostelium aggregation. Phy. D **85**, 425–444 (1995)
12. Jackson, T.L., Byrne, H.M.: A mathematical model to study the effects of drug resistance and vasculature on the response of solid tumors to chemotherapy. Math. Biosci. **164**, 17–38 (2000)
13. Janeway, C.A., Travers, P., Walport, M., Shlomchik, M.: Immuno biology. Garland, New York, 1994
14. Keller, E.F., Segel, L.A.: Model for chemotaxis. J. theor. Biol. **30**, 225–234 (1971)
15. Keller, E.F., Segel, L.A.: Traveling bands of chemotactic bacteria: a theoretical analysis. J. theor. Biol. **30**, 235–248 (1971)
16. Kirschner, D., Perelson, A.: A model for the immune system response to HIV: AZT treatment studies. In: Axelrod, A.O., Kimmel, D., and Langlais, M., (eds) Mathematical Population Dynamics: Analysis of Hetergeneity and Theory of Epidemics, Wuerz Publishing, p. 295–310 (1995)
17. Lauffenburger, D.A., Linderman, J.J.: Receptors: models for binding, trafficking, and signaling. Oxford University Press, New York, 1993
18. Lev Bar Or, R.: Feedback mechanisms between T helper cells and macrophages in the determination of the immune response. Math. Biosci. **163**, 35–58 (2000)
19. Lin, Y., Zhang, M., Barnes, P.F.: Chemokine production by a human alveola epithelial cell line in response to mycobacterium tuberculosis. Infect. Immun. **66**, 1121–1126 (1998)
20. Mayanja-Kizza, H., Johnson, J.L., Hirsch, C.S., Peters, P., Surewicz, K., Wu, M., Nalugwa, G., Mubiru, F., Luzze, H., Wajja, A., Aung, H., Ellner, J.J., Whalen, C., Toossi, Z.: Macrophage-activating cytokines in human immunodeficiency virus type 1-infected and -uninfected patients with pulmonary tuberculosis. J. Infect. Dis. **183**, 1805–1809 (2001)
21. Mims, C., Dimmock, N., Nash, A., Stephen, J.: Mims' Pathogenesis of Infectious Disease. Academic Press, New York, 1995
22. Myerscough, M.R., Maini, P.K., Painter, K.J.: Pattern formation in a generalized chemotactic model. Bull. Math. Biol. **60**, 1–26 (1998)

23. NAG Ltd.: NAG Fortran Library Manual, Mark 19 edition, 1999
24. Nathan, C.F., Murray, H.W., Wiebe, M.E., Rubin, B.Y.: Identification of interferon-gamma as the lymphokine that activates human macrophage oxidative metabolism and antimicrobial activity. J. Exp. Med. **158**, 670–689 (1983)
25. Owen, M.R., Sherratt, J.A.: Pattern formation and spatiotemporal irregularity in a model for macrophage-tumour interactions. J. theor. Biol. **189**, 63–80 (1997)
26. Owen, M.R., Sherratt, J.A.: Mathematical modelling of macrophage dynamics in tumours. Math. Models Methods Appl. Sci. **9**, 513–539 (1999)
27. Painter, K.J., Maini, P.K., Othmer, H.G.: Development and applications of a model for cellular respose to multiple chemotactic cues. J. Math. Biol. **41**, 285–314 (2000)
28. Pan, Z.K., Chen, L.-Y., Cochrane, C.G., Zuraw, B.L.: fMet-Leu-Phe stimulates proinflammatory cytokine gene expression in human peripheral blood monocytes: the role of phosphatidylinositol 3-kinase. J. Immunol. **164**, 404–411 (2000)
29. Pilyugin, S.S.: Modeling immune responses with handling time. Bull. Math. Biol. **62**, 869–890 (2000)
30. Sannomiya, P., Craig, R.A., Clewell, D.B., Suzuki, A., Fujino, M., Till, G.O., Marasco, W.A.: Characterization of a class of nonformylated enterococcus faecalis-derived neutrophil chemotactic peptides: the sex pheromones. Proc. Natl. Acad. Sci. USA **87**, 66–70 (1990)
31. Saukkonen, J.J., Bazydlo, B., Thomas, M., Strieter, R.M., Keane, J., Kornfeld, H.: β-chemokines are induced by mycobacterium tuberculosis and inhibit its growth. Infect. Immun. **70**, 1684–1693 (2002)
32. Schluger, N.W., Rom, W.N.: The host immune response to tuberculosis. Am. J. Respir. Crit. Care Med. **157**, 679–691 (1998)
33. Sherratt, J.A.: Chemotaxis and chemokinesis in eukaryotic cells: The Keller-Segel equations as an approxination to a detailed model. Bull. Math. Biol. **56**, 129–146 (1994)
34. Sherratt, J.A., Sage, E.H., Murray, J.D.: Chemical control of eukaryotic cell movement: A new model. J. theor. Biol. **162**, 23–40 (1993)
35. Sozzani, S., Luini, W., Molino, M., Jílek, P., Bottazzi, B., Cerletti, C., Matsushima, K., Mantovani, A.: The signal transduction pathway involved in the migration induced by a monocyte chemotactic cytokine. J. Immunol. **147**, 2215–2221 (1991)
36. Stout, R.D., Bottomly, K.: Antigen-specific activation of effector macrophages by IFN-gamma producing (TH1) t cell clones. failure of IL-4-producing (TH2) t cell clones to activate effector function in macrophages. J. Immunol. **142**, 760–765 (1989)
37. Tran, C.L., Jones, A.D., Donaldson, K.: Mathematical model of phagocytosis and inflammation after the inhalation of quartz at different concentrations. Scand. J. Work Environ. Health **21**, 50–54 (1995)
38. van Crevel, R., Ottenhoff, T.H.M., van der Meer, J.W.M.: Innate immunity to mycobacterium tuberculosis. Clin. Microbiol. Rev. **15**, 294–309 (2002)
39. Ward, J.P., King, J.R.: Mathematical modelling of avascular-tumour growth. IMA J. Math. Appl. Med. Biol. **14**, 39–69 (1997)
40. Ward, J.P., King, J.R.: Mathematical modelling of avascular-tumour growth ii: Modelling growth saturation. IMA J. Math. Appl. Med. Biol. **16**, 171–211 (1999)
41. WHO.: WHO Report 2001: Global Tuberculosis Control. Technical report, World Health Organization, 2001
42. Wigginton, J.E., Kirschner, D.: A model to predict cell-mediated immune regulatory mechanisms during human infection with mycobacterium tuberculosis. J. Immunol. **166**, 1951–1967 (2001)
43. Wodarz, D., Lloyd, A.L., Jansen, V.A.A., Nowak, M.A.: Dynamics of macrophage and T cell infection by HIV. J. theor. Biol. **196**, 101–113 (1999)